Available online at www.sciencedirect.com
SCIENCE DIRECT®
Biochemical and Biophysical Research Communications 300 (2003) 41–46
BBRC
www.elsevier.com/locate/ybbrc

Structure of human α_1-acid glycoprotein and its high-affinity binding site☆,☆☆

Vladimír Kopecký Jr.,[a,b,*] Rüdiger Ettrich,[c] Kateřina Hofbauerová,[b,d] and Vladimír Baumruk[a]

[a] *Institute of Physics, Charles University, Ke Karlovu 5, CZ-12116 Prague 2, Czech Republic*
[b] *Department of Biochemistry, Faculty of Science, Charles University, Albertov 2030, CZ-12840 Prague 2, Czech Republic*
[c] *Institute of Physical Biology, University of South Bohemia, Zámek 136, CZ-37333 Nové Hrady, Czech Republic*
[d] *Department of Physical and Macromolecular Chemistry, Faculty of Science, Charles University, Albertov 2030, CZ-12840 Prague 2, Czech Republic*

Received 6 November 2002

Abstract

Secondary and tertiary structures of human blood α_1-acid glycoprotein, a member of the lipocalin family, have been studied for the first time by infrared and Raman spectroscopies. Vibrational spectroscopy confirmed details of the secondary structure and the structure content predicted by homology modeling of the protein moiety, i.e., 15% α-helices, 41% β-sheets, 12% β-turns, 8% bands, and 24% unordered structure at pH 7.4. Our model shows that the protein folds as a highly symmetrical all-β protein dominated by a single eight-stranded antiparallel β-sheet. Thermal dynamics in the range 20–70 °C followed by Raman spectroscopy and analyzed by principle component analysis revealed full reversibility of the protein motion upon heating dominated by decreasing of β-sheets. Raman difference spectroscopy confirmed the proximity of Trp^{122} to progesterone binding.

Keywords: Orosomucoid; Tertiary structure; Binding site; Restraint-based homology modeling; Raman spectroscopy; Fourier transform infrared spectroscopy; Thermal stability; Progesterone binding; Principal component analysis

α_1-Acid glycoprotein (AGP), also known as orosomucoid, is a 41-kDa single polypeptide formed of 183 amino acids. It contains 42% carbohydrate in weight and has up to 16 sialic acid residues. Five heteropolysaccharide groups are linked via N-glycosidic bond to the asparaginyl residues of the protein. Two disulfide bridges are formed between cysteins 5–147 and 72–164 [1]. Chemical modification and temperature difference spectroscopy revealed that 5–7 tyrosines, 2 tryptophans [2], and almost all phenylalanines [3] are completely or partially buried in native state.

AGP, a human blood plasma protein, belongs to the lipocalin family of proteins, a heterogeneous group of extracellular proteins that bind a variety of small hydrophobic ligands. It is known that AGP plays a role under inflammatory or other pathophysiological conditions and is able to bind basic drugs, vanilloids, IgG3, heparin, and certain steroid hormones such as progesterone, however, its biological function and 3D structure remain unknown [4].

A 3D structure of AGP based on the crystal structure of the bilin-binding protein, a member of the lipocalin protein family, was proposed in 1993 [5]. Although a valuable contribution, this model has several shortcomings from nowadays view. Meanwhile the number of known X-ray structures of lipocalins significantly increased, computer technology improved, and algorithms were refined. Our approach, a combination of vibrational spectroscopy methods and molecular modeling, which, surprisingly, was not used until now, gives

☆ Dedicated to Prof. Vladimír Karpenko on the occasion of his 60th birthday.

☆☆ *Abbreviations:* AGP, α_1-acid glycoprotein; CD, circular dichroism; FTIR, Fourier transform infrared; LSA, least-squares analysis; PCA, principle component analysis; QSAR, quantitative structure–activity relationship.

* Corresponding author. Fax: +420-224-922-797.
E-mail address: kopecky@karlov.mff.cuni.cz (V. Kopecký Jr.).

0006-291X/02/$ - see front matter © 2002 Elsevier Science (USA). All rights reserved.
PII: S0006-291X(02)02765-1

detailed information about secondary structure, binding sites, and folding of AGP.

Materials and methods

Materials. The AGP was obtained from Sigma Chemical. The sample was purified by HPLC and checked by SDS electrophoresis. All other reagents used in our experiments were of analytical grade. AGP for Raman and FTIR spectroscopies was dissolved in 20 mM Tris–HCl buffer (pH 7.4) to a final concentration of 7.5 mg/ml (protein concentration was checked spectrophotometrically using the absorption coefficient $E_{1\%,1\,cm,278\,nm} = 8.93$ [6]). Progesterone diluted in ethanol was added to AGP in 1.33:1 ratio [7].

FTIR spectroscopy. Room temperature infrared spectra were recorded with a Bruker IFS-66/S FTIR spectrometer using a standard source, a KBr beamsplitter, and an MCT detector. Usually 4000 scans were collected with 4 cm^{-1} spectral resolution and a Happ–Genzel apodization function. Samples were placed in a demountable cell (Graseby Specac) consisting of a pair of CaF_2 windows and 12 μm Mylar spacer. Spectral contribution of a buffer in carbonyl stretching region was corrected following the standard algorithm [8].

Raman spectroscopy. Raman spectra were recorded on a multichannel instrument based on a 600-mm single spectrograph with a 1200-grooves/mm grating and a liquid N_2 cooled CCD detection system having 1024 pixels along dispersion axis. The effective spectral slit width was set to ~5 cm^{-1}. Samples were excited with a 514.5 nm/100 mW line of an Ar^+ laser. Calibrated wavenumber scale was accurate to ±1 cm^{-1}. Binding of progesterone, measured at 4 °C, was averaged from 300 exposures of 120 s. Thermal stability spectra were averaged from 10 exposures of 60 s. Spectra were treated according to [9]. Spectra were smoothed using 9-point Savitsky–Golay algorithm and normalized to the 1447 cm^{-1} band as an internal standard.

Principal component analysis. Principal component analysis (PCA), using a singular value decomposition algorithm, is a multivariate mathematical technique for reducing spectral data to their lowest dimension without loss of valuable information. Each spectrum can be expressed as a linear combination of loading coefficients and orthogonal subspectra. The first subspectrum corresponds to the average spectrum in studied series, whereas the following subspectra (in order of decreasing loadings, i.e., in decreasing significance) represent spectral changes. A number of significant subspectra can be estimated from singular values. (Detailed explanation can be found in [10].)

Choice of the templates and alignment. The choice of templates was restricted to the tertiary structures of lipocalin family that have been solved by X-ray crystallography. The structures 1EW3 [11], 1EPA [12], 1QQS [13], and 1A3Y [14] were extracted from the Brookhaven Protein Data Bank and structurally aligned using the SwissPDBViewer [15]. The template structures were aligned with the two genetic forms of human AGP ORS1 and ORS2 [16] by ClustalX [17] and adjusted manually according to the structural alignment. The alignment used for further modeling is shown in Fig. 1.

Modeling. The 3D models of ORS1 and ORS2 constituted by all non-hydrogen atoms were generated by Modeller6 package [18]. All the obtained models were subjected to a short simulated annealing refinement protocol available in Modeller. Finally, the tertiary structure models were checked with ProCheck [19]. ORS1 and ORS2 differ in 21 amino acids, which are of similar kind. These substitutions have no significant influence on the overall structure of AGP (root mean square deviation (C_α) being only (0.8 Å) and in the protein core region both genetic forms of AGP are fully structurally identical.

Docking procedure. The 3D crystal structure of progesterone [20] was extracted from Cambridge Structural Database [21]. Initially the substrate was placed in an arbitrary position to the binding site, which was identified by the Dock module of Sybyl (Tripos Associates). Docking into the modeled structure was performed with AutoDock [22]. The exploration of docking positions included 50 hybrid Lamarckian genetic algorithm runs using a population size of 50, and a maximum number of energy evaluations of 25,000, a maximum number of generations of 27,000 and 300 iterations of Solis and Wets' local search. The selected docking positions were subjected to 15 ps of dynamics simulation using the canonical ensemble at 300 K in Sybyl. Two thousand steps of steepest descent minimization followed, optimizing both internal and relative geometries of the substrate, and the binding site residues.

```
ORS1  ---QIPLCANLVPVPITNATLDQITGKWFYIASAFRNEEYNKSVQEIQATFFYFTPNKT-
ORS2  ---QIPLCANLVPVPITNATLDRITGKWFYIASAFRNEEYNKSVQEIQATFFYFTPNKT-
1EW3  ------------VAIRNFDISKISGEWYSIFLA---SDVKEKIEENGSMRVFVDVIRA-
1EPA  ------------AVVKDFDISKFLGFWYEIAFA---SKE---------EKMGAMVVEL-
1QQS  TSDLIPAPPLSKVPLQQNFQDNQFQGKWYVVGLA---GNAILREDK-DPQKMYATIYEE-
1A3Y  -------------------PFELSG-KWITSYIG---SSDLEKIGENAPFQVFMRSIEFD
                         .    *    .   .          .    .

ORS1  EDT-IFLREYQTRQ-DQCIY-NTTYLNVQRENGTISRYVG------GQEHFAH-LLILRD
ORS2  EDT-IFLREYQTRQ-NQCFY-NSSYLNVQRENGTVSRYEG------GREHVAH-LLFLRD
1EW3  LDNSSLYAEYQTKVNGECTE-FPMVFDKTEEDGVYSLNYD------GYNVFRI-SEFEND
1EPA  KEN-LLALTTTYYSEDHCVL-EKVTATEGDGPAKFQVTRLS-----GKKEVVV-E-ATDY
1QQS  KEDASYNVTSVLF-RKKKCDYAIRTFVPGCQPGEFTLGNIKSYPGLTSYLVRVVST--NY
1A3Y  DKESKVYLNFFSKENGICEE-FSLIGTKQEG-NTYDVNYA------GNNKFVVS--YASE
       .                                                .

ORS1  T-KTYMLAFDVN-DEKNWGL-SVYADKPE-TTKEQLGEFYEALDCLRIPKSDVVYTDWKK
ORS2  T-KTLMFGSYLD-DEKNWGL-SFYADKPE-TTKEQLGEFYEALDCLCIPRSDVMYTDWKK
1EW3  E-HIILYLVNFDK-DRPFQLFEFYAREPD-VSPEIKEEFVKIVQKRGIVKENIID-LTKI
1EPA  LTYAIIDITSLV-AGAVHRTMKLYSRSLDDNGE-ALYNFRKITSDHGFSETDLYI-LKHD
1QQS  NQHAMVFFKKVS-QNREYFKITLYGRTKE-LTSELKNNFIRFSKSLGLPENHIVF-PVP-
1A3Y  T-ALIISNINVDEEGDKTIMTGLLGKGTD-IEDQDLEKFKEVTRENGIPEENIVN-IIER
           :    .          . .   :        :* .      : . .:

ORS1  ---DKCEPLEKQHEKERKQEEGES
ORS2  ---DKCEPLEKQHEKERKQEEGES
1EW3  DRCFQLRG----------------
1EPA  LTCVKVLQSAAES-----------
1QQS  --IDQCID----------------
1A3Y  D--DCPA-----------------
```

Fig. 1. Sequence alignment of two genetic forms of AGP (ORS1, ORS2 [17]) with structures 1EW3 [11], 1EPA [12], 1QQS [13], and 1A3Y [14] whose 3D structures have been solved recently by X-ray crystallography.

Results

Secondary and tertiary structures of AGP

Interestingly, the lipocalin family is remarkably diverse at the sequence level, showing low levels of overall sequence conservation with pairwise comparisons often falling well below 20%. Despite lacking high sequence similarity, lipocalin crystal structures are characterized by a repeated +1 topology β-barrel and well conserved with a root mean square deviation value (C_α) of only 1.3–1.4 Å for the templates used. The obtained models of the two AGPs show a good quality stereochemistry, as revealed by ProCheck [19]. The torsion angles of 85% of the residues have values within the most favored regions and no residues are found in disallowed regions. The overall *g*-factor shows a value of −0.24. Ideally, the value of the *g*-factor should be above −0.5 and values below −0.1 may need further investigation. AGP folds as a highly symmetrical all-β protein dominated by a single eight-stranded antiparallel β-sheet closed back on itself to form a continuously hydrogen-bonded barrel. The eight β-strands of the barrel are linked by typical short β-hairpins except the first one: this is a large loop folded back to a lid, which partially closes the internal ligand-binding pocket found at this end of the barrel. In

the native state it contains a short α-helix that is transformed into β-sheet in the progesterone-bound state (see Table 1). Three loops are close to each other and constitute the bottom of β-barrel. Between the last strand and the C-terminus is found another α-helix, which represents an ever-present feature of the lipocalin fold (see Fig. 2).

Fig. 3 depicts the FTIR spectrum of AGP. The two major bands, observed at 1639 and 1551 cm^{-1}, are assigned to the amide I and amide II, respectively. The second derivative which can identify overlapping components reveals high content of extended β-sheets by the strong band at 1637 cm^{-1} [23]. An appearance of the second band at 1692 cm^{-1} suggests that β-sheets are antiparallel [24]. Weaker bands at 1666, 1674, and 1685 cm^{-1} belong to β-turns [23]. Characteristic amino acid side chain absorption bands can also be identified. The side chain absorbance of solvent-exposed Asp and Glu COOH modes is observable at 1700 cm^{-1}. The shoulder at 1559 cm^{-1} corresponds to stretching vibrations of COO^- of Glu. Finally, the bands at 1517 and 1617 cm^{-1} are attributed to Tyr [23].

The Raman spectrum of native AGP (Fig. 4A) can provide additional information about the structure of the protein. The band at 541 cm^{-1} corresponds to unusual *trans–gauche–trans* conformation of S–S bridges [25] which is also presented in our model for both bridges. The two bands 831 and 852 cm^{-1} are assigned to the Tyr (Y1+Y1a) Fermi resonance doublet. Its intensity ratio I_{852}/I_{831} is used as an indicator of Tyr environment [26]. The value 1.1 corresponds to 1:3 ratio of Tyr exposed to buried, i.e., three fully solvent exposed—Tyr^{74}, Tyr^{91}, and Tyr^{142}, and 8 buried Tyr residues. W17 mode of Trp at 878 cm^{-1} indicates strong NH–hydrogen bond donation [27]. The Trp Fermi doublet intensity ratio $I_{1359}/I_{1339} = 0.8$ is a sensitive marker of the amphipathic environment of the aromatic ring [27] and in our case indicates hydrophilic environment of all Trp. Direct correlation between the Raman frequency of W3 mode and the absolute value of the torsional angle $\chi^{2,1}$ is known [28]. Its position at 1552 cm^{-1} corresponds to angle $|\chi^{2,1}| = 90°$ for all Trp. In our model one torsional angle 15° for Trp^{160}, that is in a loop region on the surface of the protein and probably can be more flexible, may indicate a shortcoming of the model with respect to this loop. Other mentioned structure characteristics are presented correctly.

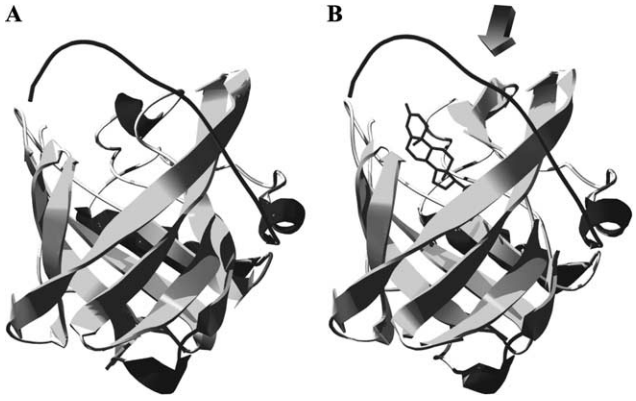

Fig. 2. The ribbon molecular model of AGP in the native state (A) shows an eight-stranded antiparallel β-barrel. It can be seen that during progesterone binding (B) the α-helix in the first loop above the β-barrel was transformed into antiparallel β-sheet (marked with an arrow).

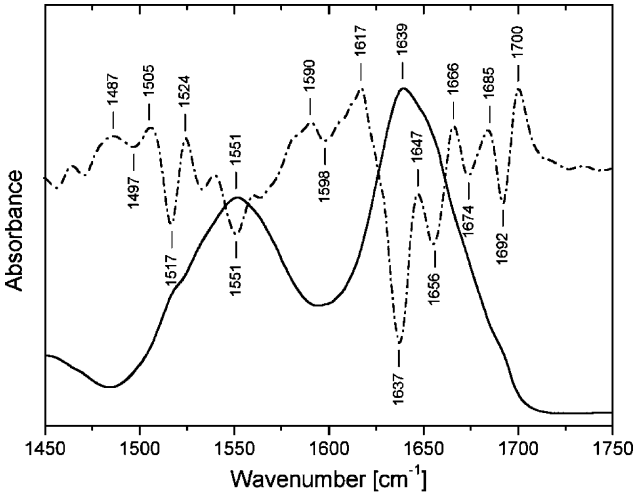

Fig. 3. The FTIR spectrum in the amide I and II regions of AGP. The solid curve represents the original spectrum while the dash-dot curve is associated with the second derivative (15 pts) of the spectrum.

Thermal dynamics of AGP

Thirty-one Raman spectra of AGP measured in a heating–cooling and the second heating cycle were analyzed by PCA (data not shown). PCA revealed full reversibility and two different types of behaviors were observed. The following spectral regions were analyzed

Table 1
Secondary structure estimation (in percentage) of AGP by FTIR and Raman spectroscopies compared with the model structure

Method	AGP					AGP binding progesterone				
	α-Helix	β-Sheet	β-Turn	Bend	Other	α-Helix	β-Sheet	β-Turn	Bend	Other
Model	15	41	12	8	24	12	44	12	8	24
FTIR-LSA[a]	12	37	13	15	25	9	41	14	11	26
Raman-LSA[b]	14	42	20	–	28	10	47	20	—	28

[a] Least-squares analysis of FTIR amide I and amide II bands according to [36].
[b] Least-squares analysis of Raman amide I band according to [9].

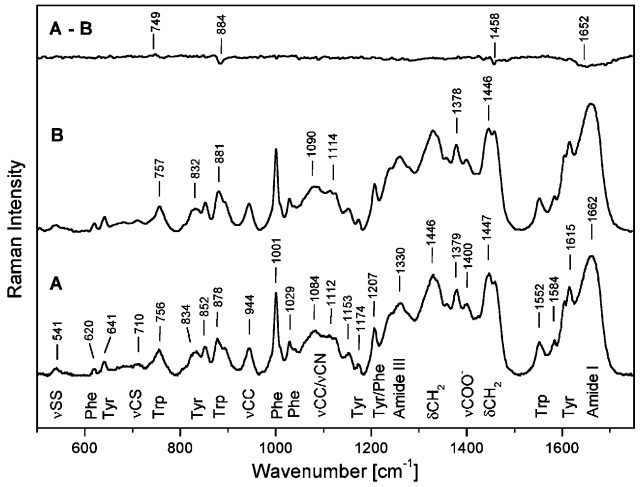

Fig. 4. A comparison of the Raman spectra of AGP (A) and AGP with bound progesterone (B). The spectrum A–B represents the difference caused by binding. The assignment of the bands is discussed in the text (ν corresponds to stretching and δ to bending vibrations).

by PCA independently and only two subspectra were found to be significant. The second loading coefficient revealed strong linear dependence on temperature for Trp band 878 cm^{-1} and for the hide band at 1165 cm^{-1}. The same but weaker dependence was also observed for νCS vibrations at 670 cm^{-1}, νCC/νCN at ca. 1110 cm^{-1}, νCOO^- at 1379 cm^{-1}, and Trp bands 1552 cm^{-1}. This type of behavior corresponds to motions on the periphery or on the most flexible unordered parts of the protein. On contrary, a very complex type of motion was found in amide I region. PCA showed that three subspectra are significant. The second subspectrum resembles β-sheet spectrum (max. at 1675 cm^{-1}) and its loading shows decrease of the β-sheet content with increasing temperature starting at ca. 50 °C. Thus it is probably "breathing" of β-barrel. However, the third subspectrum is similar to β-turns and random coil structure (max. at 1665 cm^{-1}). Its coefficient showed very complex behavior and thus corresponds to complicated rearrangement connected with "breathing" of β-barrel.

Second derivative of FTIR spectra of AGP exposed to a heat shock of 70 °C shows one significant difference in comparison to spectrum of native AGP (data not shown). The shoulder at 1559 cm^{-1} (see Fig. 3), corresponding to νCOO^- of Glu residues, disappeared after heat shock. Thus, probably on the periphery of AGP irreversible structural change of the protein exists. Nevertheless, this spectral change is also accompanied with a downshift of the 1617 cm^{-1} band to 1612 cm^{-1}. This might be attributed to the presence of little amount of β-aggregated protein after heat shock.

Progesterone binding

Docking of progesterone into the hydrophobic binding-pocket of AGP shows that during progesterone

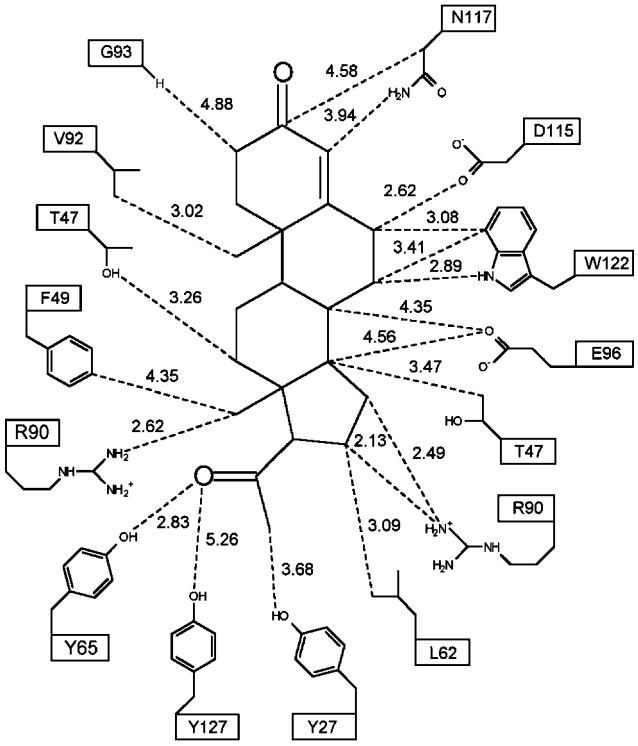

Fig. 5. Schematic representation of progesterone–AGP interactions in the central hydrophobic pocket of the protein. Distances are in Å; one letter code and amino acid number are indicated for side chains involved.

binding the α-helix above the β-barrel was transformed into antiparallel β-sheet, see Fig. 2. This effect is in good agreement with spectroscopic determination of changes in the secondary structure caused by progesterone binding (see Table 1). However, the most interesting results were revealed by Raman difference spectroscopy, see Fig. 4. Slight changes in the amide I region (about 1652 cm^{-1}) fully correspond to rearrangement in the secondary structure of AGP. Spectral changes of δCH_3 vibrations (ca. 1458 cm^{-1}) can be interpreted as local change of AGP caused by progesterone binding. The shift of the W17 mode at 882 cm^{-1} indicates changes in Trp NH–hydrogen bond donation that corresponds to proximity of Trp^{122} to the progesterone binding site in our model structure, as shown in Fig. 5. Computer docking explored two positions for progesterone in the huge hydrophobic cavity inside the β-barrel differing only by 0.5 kcal/mol. Raman spectra did not reveal any changes in the environment of Tyr, thus only the position depicted in Fig. 5 is allowed. Progesterone in the opposite orientation would strongly interact with Tyr^{27} and Tyr^{127}, which was not observed.

Discussion

Our estimation of α-helical content is higher (see Table 1) than was determined by circular dichroism

(CD) measurements in [29], i.e., 8% of α-helix, 60% of β-sheets, and 10% of β-turn. Strong disagreement can be seen for β-sheets which [29] overestimates by about 20%. This shortcoming of CD can be easily explained. β-Sheets are determined with the highest error in CD spectroscopy of proteins. In all works presented, the secondary structure content of AGP by CD [29,30] was not discussed with regard to affecting of CD spectra by saccharide moiety of the protein. It was demonstrated by partial deglycosylation of AGP [30], which leads to decreasing of β-sheet to approximately 20%, however, a thermal stability of the protein was not influenced. It is not probable that such an extensive rearrangement of protein did not have influence on thermal stability. Thus, we can conclude the fact that the error is mostly caused by the presence of sialic acid residues which did not affect the estimation from the vibrational spectra.

Observation of the decreasing of β-sheets in AGP upon heating as well as full reversibility after the heat shock is in agreement with results from CD spectroscopy [29]. The behavior of AGP in the heating cycle did not reveal any indications of the protein core rearrangement in contrast with the behavior at low pH [31]. Trp thermal dynamics of W17 mode at 877 cm^{-1} suggest high sensitivity to little conformational changes of AGP. Thus, it seems to be impossible to mark the band at ca. 880 cm^{-1} as diagnostic, as was proposed in [32], for sialylation of AGP as well as diagnostic for sialylation in proteins generally because desialylation cause conformational changes on which sensitively react Trp residues.

Whereas in an earlier study [5], binding site residues were identified only by superposition of substrate–ligand complexes of lipocalin family members with the modeled structure, we are the first to report the real computer docking of a ligand into the binding pocket. General physico-chemical properties of the binding pocket are in good agreement with those determined by QSAR methods [33]. Connection of molecular modeling with Raman spectroscopy enabled us to identify the high-affinity binding site residues of AGP precisely (see Fig. 5). Our finding that Trp^{122} residue is in the binding site is in excellent agreement with fluorescence measurements that reported a distance between Trp and progesterone lower than 5.5 Å [34] and an influence of progesterone binding on Trp [7]. In contrast, Förster's radiationless energy transfer led to a distance of about 9.1–14.1 Å [35], whereas the average distance between the π electron systems is not greater than 7 Å in our model. Lys^{39} in our model is located within the short α-helical segment on the loop closing partially the binding-pocket, which is transformed into β-sheet during binding. This plausibly explains the fact that a chemical modification of at least one lysine residue by phenylisocyanate and naphthylisocyanate leads to a reduction of progesterone binding ability as reported in [35]. The presence of Tyr^{27} and Tyr^{65} deep in the binding pocket explains the fact that progesterone in the binding site protects up to two Tyr residues from nitration by tetranitromethane [35].

Finally, our model was verified in so many details by vibrational spectroscopy that the model structure brings valuable contribution to understanding the structure of AGP and specially its ability to bind different small hydrophobic molecules. A model of the protein moiety of AGP in native state and with docked progesterone in PDB-format is available upon request.

Acknowledgments

The authors thank Dr. R. Hampl (Institute of Endocrinology, Czech Republic) for a kind gift of the progesterone sample. The support by the Grant Agency of the Charles University (No. 220/2000/B-CH) and the Ministry of Education of the Czech Republic (No. MSM113100001, No. MSM 113200001, No. MSM123100001) is acknowledged.

References

[1] K. Schmid, H. Kaufmann, S. Isemura, F. Bauer, J. Emura, T. Motoyama, M. Ishiguro, S. Nanno, Structure of α_1-acid glycoprotein. The complete amino acid sequence, multiple amino acid substitutions, and homology with immunoglobulins, Biochemistry 12 (1973) 2711–2724.

[2] K. Schmid, L.H. Chen, J.C. Occhino, E.A. Foster, K. Sperando, Topography of human plasma α_1-acid glycoprotein, Biochemistry 15 (1976) 2245–2255.

[3] L. Janáčková, V. Karpenko, Thermal stability of human blood serum orosomucoid (α_1-acid glycoprotein) in water–ethanol systems, Collect. Czech. Chem. Commun. 59 (1994) 2190–2200.

[4] T. Fournier, N. Medjoubi-N, D. Porquet, α-1-acid glycoprotein, Biochim. Biophys. Acta 1482 (2000) 157–171.

[5] A. Rojo-Domínguez, A. Hernández-Arana, Three-dimensional modeling of the protein moiety of human α_1-acid glycoprotein, a lipocalin-family member, Protein Seq. Data Anal. 5 (1993) 349–355.

[6] H.E. Schulze, J.F. Heremans, in: Molecular Biology of Human Proteins, Elsevier, Amsterdam, 1966, p. 203.

[7] J.R. Albani, Binding effect of progesterone on the dynamics of α_1-acid glycoprotein, Biochim. Biophys. Acta 1336 (1997) 349–359.

[8] F. Dousseau, M. Therrien, M. Pézolet, On the spectral subtraction of water from the FT-IR spectra of aqueous solutions of proteins, Appl. Spectrosc. 43 (1989) 538–542.

[9] R.W. Williams, Protein secondary structure analysis using Raman amide I and amide III spectra, Methods Enzymol. 130 (1986) 311–331.

[10] E.R. Malinowski, Factor Analysis in Chemistry, second ed., Wiley, New York, 1991.

[11] M.B. Lascombe, C. Gregoire, P. Poncet, G.A. Tavares, I. Rosinski-Chupin, J. Rabillon, H. Goubran-Botros, J.C. Mazie, B. David, P.M. Alzari, Crystal structure of the allergen equ C 1. A dimeric lipocalin with restricted ige-reactive epitopes, J. Biol. Chem. 275 (2000) 21572–21577.

[12] M.E. Newcomer, Structure of the epididymal retinoic acid binding protein at 2.1 Å resolution, Structure 1 (1993) 7–18.

[13] D.H. Goetz, S.T. Willie, R. Armen, T. Bratt, N. Borregaard, R.K. Strong, Ligand preference inferred from the structure of neutrophil gelatinase associated lipocalin, Biochemistry 39 (2000) 1935–1941.

[14] S. Spinelli, R. Ramoni, S. Grolli, J. Bonicel, C. Cambillau, M. Tegoni, The structure of the monomeric porcine odorant binding protein sheds light on the domain swapping mechanism, Biochemistry 37 (1998) 7913–7918.
[15] N. Guex, M.C. Peitsch, SWISS-MODEL and the Swiss-Pdb-Viewer: An environment for comparative protein modeling, Electrophoresis 18 (1997) 2714–2723.
[16] L. Dente, M.G. Pizza, A. Metspalu, R. Cortese, Structure and expression of the genes coding for human alpha 1-acid glycoprotein, EMBO J. 6 (1987) 2289–2296.
[17] J.D. Thompson, T.J. Gibson, F. Plewniak, F. Jeanmougin, D.G. Higgins, The CLUSTAL_X windows interface: flexible strategies for multiple sequence alignment aided by quality analysis tools, Nucleic Acids Res. 25 (1997) 4876–4882.
[18] A. Sali, T.L. Blundell, Comparative protein modelling by satisfaction of spatial restraints, J. Mol. Biol. 234 (1993) 779–815.
[19] R.A. Laskowski, M.W. McArthur, D.S. Moss, J.M. Thornton, Procheck—a program to check the stereochemical quality of the protein structures, J. Appl. Crystallogr. 26 (1993) 283–291.
[20] H. Campsteyn, L. Dupont, O. Dideberg, Structure cristalline et moléculaire de la progestérone, Acta Cryst. B 28 (1972) 3032–3042.
[21] F.H. Allen, O. Kennard, 3D search and research using the cambridge structural database, Chem. Design Autom. News 8 (1993) 31–37.
[22] G.M. Morris, D. Goodsell, R. Huey, A.J. Olson, Distributed automated docking of flexible ligands to proteins: Parallel applications of AutoDock 2.4, J. Comput. Aided-Mol. Design 10 (1996) 293–304.
[23] H. Fabian, W. Mäntele, Infrared spectroscopy of proteins, in: J.M. Chalmers, P.R. Griffiths (Eds.), Handbook of Vibrational Spectroscopy, Wiley, Chichester, 2002, pp. 3399–3425.
[24] N. Yamada, K. Ariga, M. Naito, K. Matsubara, E. Koyama, Regulation of β-sheet structures within amyloid-like β-sheet assemblage from tripeptide derivatives, J. Am. Chem. Soc. 120 (1998) 12192–12199.
[25] H.E. Van Wart, H.A. Scheraga, Raman spectra of strained disulfides. Effect of rotation about sulfur-sulfur bonds on sulfur-sulfur stretching frequencies, J. Phys. Chem. 80 (1976) 1823–1832.
[26] M.N. Siamwiza, R.C. Lord, M.C. Chen, Interpretation of the doublet at 850 and 830 cm^{-1} in the Raman spectra of tyrosyl residues in proteins and certain model compounds, Biochemistry 14 (1975) 4870–4876.
[27] T. Miura, H. Takeuchi, I. Harada, Characterization of individual tryptophan side chains in proteins using Raman spectroscopy and hydrogen–deuterium exchange kinetics, Biochemistry 27 (1988) 88–94.
[28] T. Miura, H. Takeuchi, I. Harada, Tryptophan Raman bands sensitive to hydrogen bonding and side-chain conformation, J. Raman Spectrosc. 20 (1989) 667–671.
[29] M. Kodíček, A. Infanzón, V. Karpenko, Heat denaturation of human orosomucoid in water–methanol mixtures, Biochim. Biophys. Acta 1246 (1995) 10–16.
[30] S. Šebánková, V. Karpenko, G. Entlicher, The effect of partial deglycosylation on the structure of α_1-acid glycoprotein, Gen. Physiol. Biophys. 18 (1999) 371–386.
[31] K. Hofbauerová, V. Kopecký Jr., J. Sýkora, V. Karpenko, Thermal stability of the human blood serum acid α_1-glycoprotein in acidic media, Biophys. Chem. 103 (2003) 23–31.
[32] V. Oleinikov, E. Kryukov, M. Kovner, M. Ermishov, A. Tuzikov, S. Shiyan, N. Bovin, I. Nabiev, Sialylation sensitive bands in the Raman spectra of oligosaccharides and glycoproteins, J. Mol. Struct. 480-481 (1999) 475–480.
[33] F. Hervé, G. Caron, J.-C. Duché, P. Gaillard, N.B. Rahman, A. Tsantili-Kakoulidou, P.-A. Carrupt, P. D'Athins, J.-P. Tillement, B. Testa, Ligand specificity of the genetic variants of human α_1-acid glycoprotein: generation of three-dimensional quantitative strucuture-activity relationship model for drug binding to the A variant, Mol. Pharmacol. 54 (1998) 129–138.
[34] S.D. Stroupe, S.-L. Chang, U. Westphal, Fluorescence quenching of progesterone-binding globulin and α_1-acid glycoprotein upon binding of steroids, Arch. Biochem. Biophys. 168 (1975) 473–482.
[35] T. Kute, U. Westphal, Chemical modification of α_1-acid glycoprotein for characterization of the progesterone binding site, Biochim. Biophys. Acta 420 (1976) 195–213.
[36] F. Dousseau, M. Pézolet, Determination of the secondary structure content of proteins in aqueous solutions from their amide I and amide II infrared bands. Comparison between classical and partial least-squares methods, Biochemistry 29 (1990) 8771–8779.